Doping Effect of Organic Sulphonic Acids on the Solid-State Synthesized Polyaniline

Tursun Abdiryim,[1,2] Ruxangul Jamal,[1] Ismayil Nurulla[1,2]

[1]*Key Laboratory of Petroleum and Gas Fine Chemicals, Educational Ministry of China, School of Chemistry and Chemical Engineering, Xinjiang University, Urumqi 830046, People's Republic of China*
[2]*School of Science, Xi'an Jiaotong University, Xi'an 710049, China*

Received 12 October 2006; accepted 10 January 2007
DOI 10.1002/app.26070
Published online 27 March 2007 in Wiley InterScience (www.interscience.wiley.com).

ABSTRACT: Polyaniline (PANI) salts doped with organic sulfonic acids (methanesulfonicacid, *p*-toluenesulphonic acid, and dodecylbenzenesulphonic acid) were first synthesized by using solid-state polymerization method. The polymers were characterized by Fourier transform infrared (FTIR) spectra, ultraviolet-visible spectrometry, X-ray diffraction, cyclic voltammetry, scanning electron microscopy, transmission electron microscopy, and conductivity measurements. It was found that PANI doped with *p*-toluenesulphonic acid is formed in conductive emeraldine oxidation state, and displayed higher doping level and cyrstallinity. On the contrary, PANI doped with dodecylbenzenesulphonic acid was lower at doping level and highly amorphous. In accordance with these results, the conductivity and electrochemical acitivity was also found to be higher in *p*-toluenesulphonic acid-doped PANI, and these properties were opposite in the case of dodecylbenzenesulphonic acid. The results also revealed that the morphology of dodecylbenzenesulphonic acid-doped PANI was remarkably different from other PANI salts. © 2007 Wiley Periodicals, Inc. J Appl Polym Sci 105: 576–584, 2007

Key words: conducting polymer; polyaniline; solid-statepolymerization; organic sulfonic acids

INTRODUCTION

Among conducting polymers, studies on polyaniline (PANI) have been very attractive and interesting because of its high conductivity, good redox reversibility and stability in aqueous solutions and air for its applications and in electrochromic displays, electrocatalysis, rechargeable batteries, and sensors.[1–7] PANI can be synthesized by either chemically or electrochemically oxidative polymerization as a bulk powder or film. Many papers dealing with the synthesis of PANI have been published.[8–10] The classical chemical synthesis of PANI is carried out in solution using aniline, an oxidant, and a strong doping acid with either aqueous or organic solvents.[11] Since the liquid monomer aniline forms solid salts with doping acids, room-temperature solid-state polymerization of aniline is possible using a solid anilinium salt as the precursor. Gong et al. have reported solid state synthesis of PANI doped with $H_4SiW_{12}O_{40}$ under $-20^{\circ}C$ by furbishing in mortar,[12] and Kaner and coworkers have reported solvent-free mechanochemical route to PANI in which the reaction is induced by ball-milling an anilinium salt and an oxidant under ambient conditions.[13,14] Solid-state synthesis method is, however, advantageous; the reactant molecule is put in order in solid-state synthesis reaction and the reaction happens on the surface of reactant molecule only, and this will bring some special properties of PANI material. In this report, attempt was made to understand the relations between dopant and characteristics of solid-state synthesized PANI by varying the protonation media [methanesulphonic acid (MeSA), *p*-toluenesulphonic acid, and dodecylbenzenesulphonic acid]. We want to focus here on how the oxidation state, doping level, cyrstallinity, electrochemical activity, morphology, and conductivity of the solid-state synthesized PANI change by varying the organic sulfonic acids to illuminate the relations between molecular structure, molecular size, and acidity constants (p*K*a) of these organic sulfonic acids and physicochemical characteristics of PANI salts. Thus, in a systematic approach, a comparison of the characteristics of PANI salts was done by Fourier transform infrared (FTIR) spectra, ultraviolet-visible (UV–vis) spectrometry, X-ray diffraction, cyclic voltammetry (CV), scanning electron microscopy (SEM), transmission electron microscopy (TEM), and conductivity measurements. The results were discussed with respect to

Correspondence to: I. Nurulla (Ismayilnu@sohu.com).
Contract grant sponsor: National Natural Science Foundation of China; contract grant numbers: 20274035, 20674066.
Contract grant sponsor: Xinjiang University; contract grant number: 100096.

Journal of Applied Polymer Science, Vol. 105, 576–584 (2007)

possible correlations between physicochemical characteristics of polymers and the identity of the dopant being present during the solid-state polymerization.

EXPERIMENTAL

Synthesis

Aniline and ammonium peroxydisulfate (APS) of analytical-reagent grade were obtained from Xi'an Chemical Reagent Company (China). Methyl sulfonic acid, *p*-toluene sulfonic acid, and dodecylbenzenesulphonic acid were obtained from Acros Organics. Aniline was purified by distillation. All other chemicals and solvents were used as received without further purification.

A typical solid-state polymerization procedure was as followed:[15] 1 mL of distilled water and 1.44 g MeSA were put in the mortar, they were grinded to mix each other, and then freshly distilled 1 mL of aniline was added dropwise. After grounding the reactant about 10 min, the mixture became white paste; 2.2 g of APS was added by further grounding for 30 min until the color of solid changed to black green. The greenish black powder was washed with ethylether, ethanol, and distilled water, respectively, until the filtrate was colorless, and then the powder dried under vacuum at 50°C for 48 h.

PANI salts with dodecylbenzenesulphonic acid (PANI-DBSA) and *p*-toluene sulfonic acid (PANI-*p*-TSA) as dopant were synthesized in the similar manner.

Characterization

FTIR spectra of the polymers were obtained by using a BRUKERQEUINOX-55 FTIR spectrometer (Billerica, MA) (frequency range 3500–400 cm^{-1}). UV–vis spectra of the polymer solution in *m*-cresol were recorded by using HITACHI-U3010 double beam spectrophotometer (Tokyo, Japan) in the range of 300–900 nm. The X-ray diffraction studies were performed on a D/Max 2400 X-ray diffractometer (Tokyo, Japan) by using CuKα radiation source ($\lambda = 0.15418$ nm). The scan range (2θ) was 10°–70°. The CV was performed with a CHI 660A Electrochemical Workstation (CH Instruments, USA) in a conventional three-electrode cell; the working electrode was a PANI film electrode prepared by casting the DMF solution of respective PANI salts on platinium electrode. The reference electrode was SCE, and the counter electrode was a 1 cm^2 area Pt flag. SEM images of the polymers were observed with a Leo1430VP microscope operating at 20 kV, after the polymers were gold-coated. The TEM studies of the polymer were carried out in a TEM apparatus (Hitachi, H-600). The electrical conductivity measurements were made on 1-cm-diameter pellets of the samples at 25°C, using a SDY-IV four-probe instrument.

RESULTS AND DISCUSSION

IR spectroscopy studies

Figure 1 shows the FTIR spectra of PANI salts synthesized by solid-state synthesis method; the bands assignments are summarized in Table I. The characteristic bands at $\sim$ 2916–2949 cm^{-1} can be assigned to the stretching vibration methyl ($—CH_3$) group. The two bands appearing at $\sim$ 1565–1569 cm^{-1} and $\sim$ 1487–1497 cm^{-1} can be ascribed to the stretching vibration of quinoid and benzenoid ring, respectively. The bands at $\sim$ 1297–1301 cm^{-1} can be assigned to the C—N mode, while the bands at $\sim$ 1121–1140 cm^{-1} were the characteristic bands of stretching vibration of quinoid. The bands appearing at $\sim$ 798–814 cm^{-1} were attributed to an aromatic C—H out-of-plane bending vibration.[15–17] The presence of $—SO_3^-$ group was confirmed by the appearance of bands around $\sim$ 567–588, $\sim$ 1005–1008, and $\sim$ 1031–1039 cm^{-1} in all spectra of PANI salts.[16–18] The presence of vibration band of the dopant ion and other characteristic bands confirmed that the PANI salts contain the conducting emeraldine salt phase.

The presence of bands at $\sim$ 1565–1569 cm^{-1} and $\sim$ 1487–1490 cm^{-1} clearly showed that the polymer was composed of amine and imine units. Further, it gave support to an earlier prediction of the presence of different oxidation states of the polymer. The relative intensities of these bands points toward the oxidation state of the polymer.[19] A comparison of the relative intensity of quinoid to benzenoid ring modes ($I_{\sim 1565–1569}/I_{\sim 1487–1490}$) showed the highest ratio of $\sim$ 1.0 in *p*-TSA compared to DBSA and MeSA

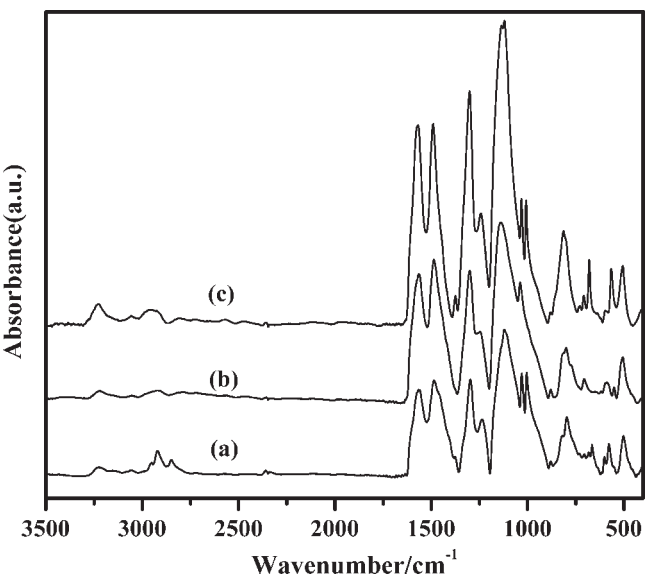

Figure 1 FTIR spectra of (a) PANI-DBSA, (b) PANI-MeSA, (c) PANI-*p*-TSA.

TABLE I
Band Wavenumber and Assignments of the PANI Salts

Band position (cm^{-1})			
PANI-DBSA	PANI-MeSA	PANI-*p*-TSA	Assignment[a]
578	588	567	νS=O
798	801	814	γCH
1005	–	1008	δCH, νS=O
1031	1039	1032	γC-CH_3, νS=O
1121	1140	1121	δCH
1297	1301	1301	νCN
1490	1487	1490	νCC
1566	1565	1569	νCC + νQN
2916	2920	2949	νCH_3
3228	3221	3228	νNH_2^+, NH^+, νNH

[a] Q denotes quinoid units of the polymers; ν, stretching mode; δ, bending mode; γ, deformation mode.

(Table II), which indicated that the emeraldine (half-oxidized form) type structure was predominant in PANI-*p*-TSA, and reduced phase were predominant in PANI-DBSA and PANI-MeSA.

It has already been reported that the higher pH value of the reaction medium and oxidant concentration will lead to higher oxidation state of PANI.[20] Therefore, it was reasonably deduced that the different oxidation state of these PANI salts were resulted from different pH value. Another considerable effect on the oxidation state of these PANI salts may be the different molecular size of each acid in solid-state polymerization, which led to separation of oxidant (APS) from monomer (aniline salt); this would in turn cause different oxidant concentration.

In this case, all the dopants studied (Table III) were in the same mole (0.015 mol); the pH value may be different with pK_a values of organic sulfonic acids and the small amount of water in reaction medium. Among the dopants, based on the pK_a values given in Table III, *p*-TSA was the most basic (the acid strength is decreased, as the p*K*a value is increased). However, the pH value of reaction medium also related to the solubility of these organic acids in water, which led to different $[H^+]$. It is well known from the literature that the water solubility of these organic sulfonic acids decreased in the order: MeSA > *p*-TSA > DBSA; this meant that most strong acidic medium occurred in the case of MeSA. As a result, the strong acidity and smaller molecular

TABLE II
Relative Intensity of Quinoid to Benzenoid Ringmodes of the PANI Salts

Sample	$I_{\sim1565-1569}/I_{\sim1487-1490}$
PANI-DBSA	0.92
PANI-MeSA	0.90
PANI-*p*-TSA	1.0

TABLE III
Acidity Constants (p*K*a) of Acids Used in Present Study[18, 21,22]

Type of acid	Abbreviation	Acidity constant (p*K*a)
methanesulphonic acid	MeSA	−1.8
p-toluenesulphonic acid	*p*-TSA	1.7
dodecylbenzenesulphonic acid	DBSA	−6.0

size of MeSA would favor the formation reduction state of PANI during the oxidative polymerization. But for *p*-TSA, the lower acidity than that of MeSA would cause the more oxidative state of PANI; this may be because emeraldine type structure is predominant in PANI-*p*-TSA. In contrast with other organic sulfonic acids, DBSA has larger molecular size and lower solubility in water for its longer alkyl chain length. The lower water solubility would lead to lower the $[H^+]$, which would favor the formation oxidation state of PANI, but the separation of oxidant (APS) from monomer (aniline salt) would be caused by steric hindrance of longer alkyl chain length of DBSA, which was also of benefit for reduction state of PANI during the oxidative polymerization. As the result of two opposite effects, the relative intensity of quinoid to benzenoid ring modes of PANI-DBSA showed between that of PANI-*p*-TSA and PANI-MeSA.

UV–vis spectroscopy studies

Figure 2 represents the UV–vis absorption spectra of PANI salts synthesized by solid-state synthesis method, in *m*-cresol solution. These PANI salts showed three characteristic absorption peaks at

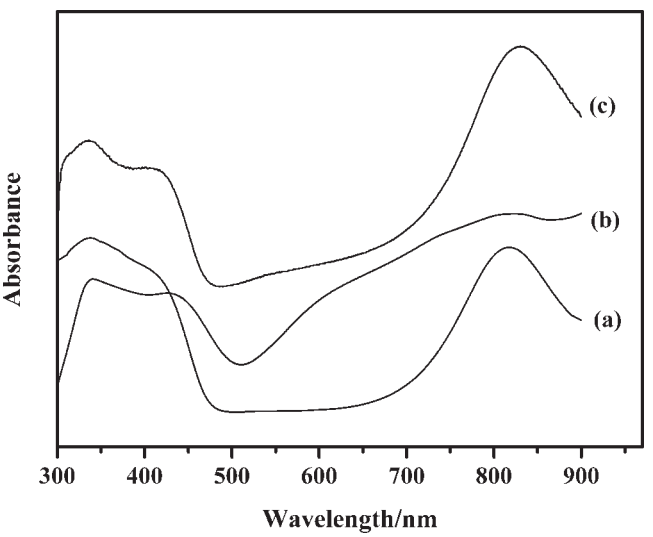

Figure 2 UV–vis spectra of (a) PANI-DBSA, (b) PANI-MeSA, (c) PANI-*p*-TSA.

TABLE IV
The Assignments of UV–vis Absorption Peaks of POT Salts

Polymer	Wave length of absorption peak			
	π–π^* transition	polaron–π^* transition	π–polaron transition	$A_{820–830}/A_{336–342}$
PANI- *p*-TSA	336 nm	416 nm	830 nm	1.40
PANI-MeSA	342 nm	424 nm	821 nm	1.22
PANI- DBSA	338 nm	405 nm	820 nm	0.95

$\sim$ 336–342, $\sim$ 405–424, and $\sim$ 821–830 nm (Table IV). The absorption peak at $\sim$ 336–342 nm can be ascribed to π–π^* transition of the benzenoid rings, whereas the peaks at 405–424 and 821–830 nm can be attributed to polaron–π^* transition and π–polaron transition, respectively[23–25]; furthermore, the peaks at $\sim$ 405–424 and $\sim$ 820–830 nm were related to doping level and formation of polaron.[25] Based on the previous research that the extent of doping can roughly be estimated from the absorption spectra of the PANI, in which the ratio of absorbances at 821–830 nm and 336–342 nm indicated the doping level of PANI,[26–28] it was found that the intensity ratio ($A_{821–830}/A_{336–342}$) was smallest in PANI-DBSA, which meant that the doping level of PANI-DBSA was lower than that of PANI-*p*-TSA and PANI-MeSA. This difference may result from bigger molecular size, especially the longer alkyl chain length that of DBSA. In solid-state synthesis method, the doping level of PANI depends on the ability of dopant to penetrate into the polymer chain. The bigger the steric hindrance dopant has, the lower the doping degree of PANI is. In addition, relative intensity of quinoid to benzenoid ring modes showed the smaller ratio of 0.92 in PANI-DBSA. This implied that there is a smaller portion of the quinoid structural units in PANI-DBSA molecular chains; therefore, the doping level decreased with the decrease of the oxidation degree of the PANI.

XRD analysis

The X-ray diffraction patterns for the PANI powder obtained through solid-state synthesis method doping with different organic sulfonic acid are shown in Figure 3. The detailed data are presented in Table V. The Bragg

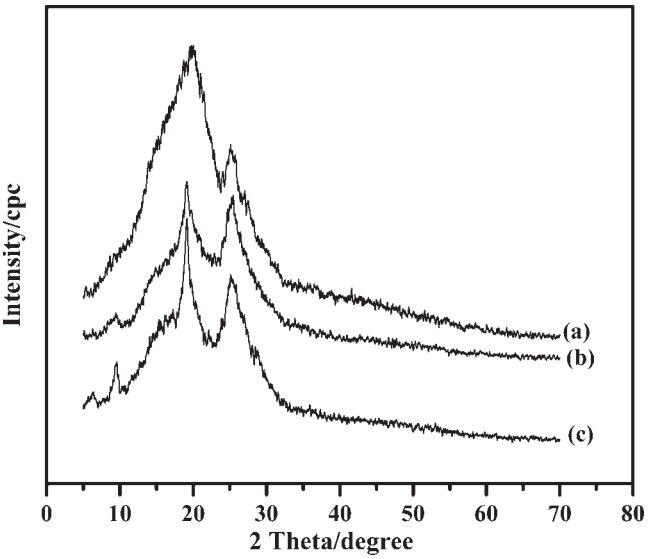

Figure 3 XRD patterns of (a) PANI-DBSA, (b) PANI-MeSA, (c) PANI-*p*-TSA.

diffraction peaks of 2θ $\sim$ 9.5°(d $\sim$ 9.302 Å), $\sim$ 19°(d $\sim$ 4.633–4.648 Å), and 25°(d $\sim$ 3.504–3.531 Å) can be found in the X-ray diffraction patterns of the PANI-MeSA and PANI-*p*-TSA, while two peaks centered at 2θ $\sim$ 19.90°(d $\sim$ 4.458 Å) and $\sim$25.16°(d $\sim$ 3.537 Å) were observed in the case of PANI-DBSA.

The peak at lowest angle [2θ $\sim$ 9.5°(d $\sim$ 9.302 Å)] was considered to be the distance between two stacks in the 2D stacking arrangement of polymer chains with intervening dopant ions between stacks,[29] and the peak centered at 2θ $\sim$ 19.08–19.90° may be ascribed to periodicity parallel to the polymer chain, while the peaks at 2θ $\sim$ 25.16–25.40° may be caused by the periodicity perpendicular to the polymer chain.[30] The peak at 2θ $\sim$ 25.16–25.40° also represented the characteristic distance between the ring planes of benzene rings in adjacent chains or the close-contact interchain distance.[31,32] It was discernible from the figure and table that the peak of 2θ $\sim$ 25.16–25.40° was weaker than that of 2θ $\sim$ 19.08–19.90° in PANI salts, which was similar to that of less doped emeradine salt.[33] To contrast with other PANI salts, the peak of 2θ $\sim$ 19.90° was stronger than that of 2θ $\sim$ 25.16° in PANI-DBSA, and PANI-DBSA exhibited a broad amorphous peak. Further, the

TABLE V
XRD Data of PANI Salts

	2θ(intensity)				
PANI-DBSA	d (Å)	PANI-MeSA	d (Å)	PANI- *p*-TSA	d (Å)
–	–	9.50° (w)	9.302	9.50° (w)	9.302
19.90° (s)	4.458	19.08° (m)	4.648	19.14° (s)	4.633
25.16° (w)	3.537	25.40° (m)	3.504	25.20° (m)	3.531

s, strong; w, weak; m, medium.

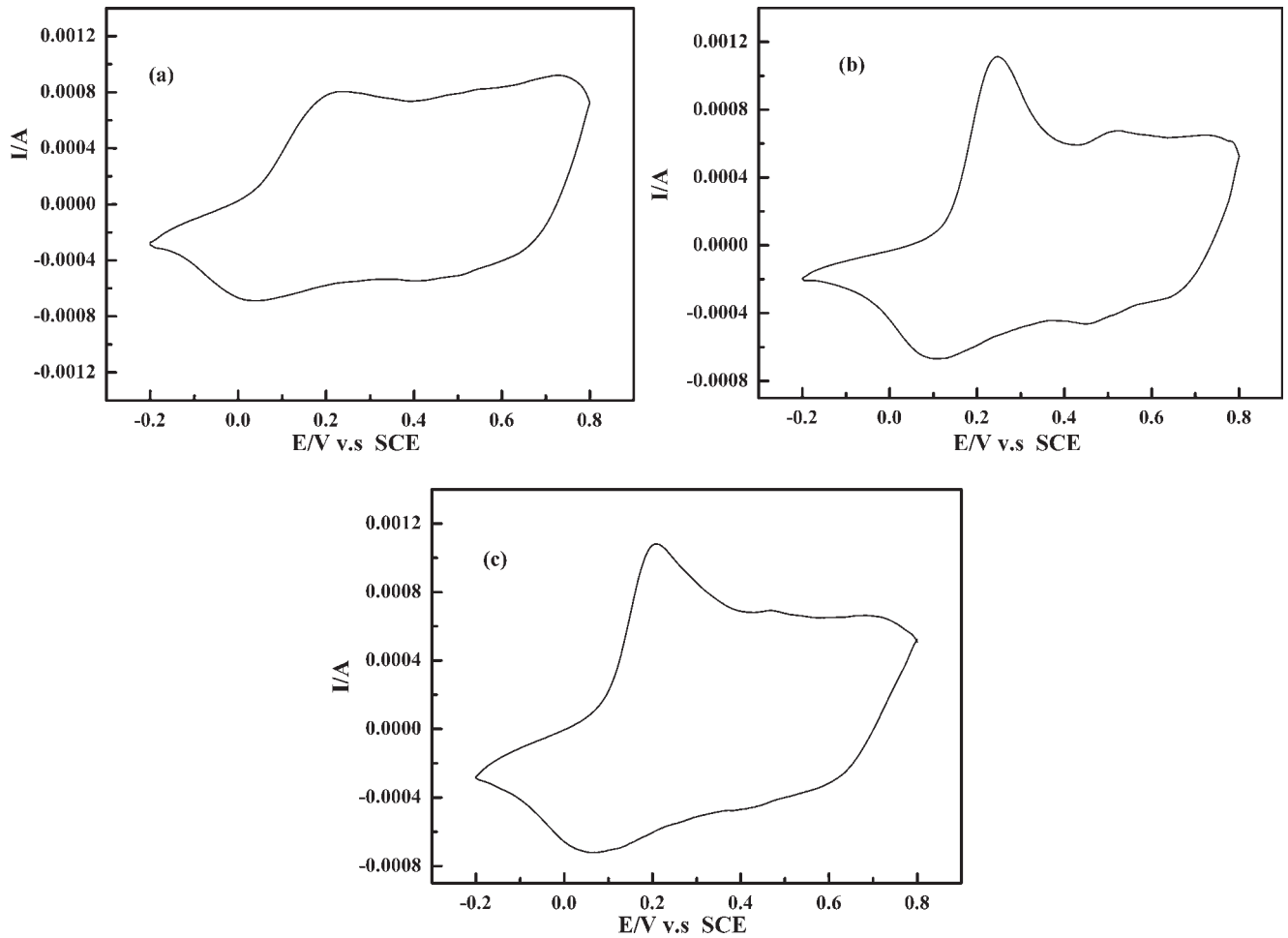

Figure 4 Cyclic voltammograms of (a) PANI-DBSA, (b) PANI-MeSA, (c) PANI-*p*-TSA in 1 mol/L H_2SO_4 solution scan rate: 50 mV/s.

d-space corresponding to the peak at $2\theta \sim 25.16$–25.40° was in the order of PANI-MeSA > PANI- *p*-TSA > PANI- DBSA. These differences did offer some inferences with regard to the effects of these organic sulfonic acids on the structural aspects of PANI. Generally, the crystallinity of PANI increases with the doping level, such an effect can be explained by the fact that the insertion of doping anions between polymer chains makes the polymer structure more rigid and favors the crystalline state,[33,34] for PANI-DBSA, the lower doping degree of DBSA in PANI and longer alkyl tail of DBSA would make PANI more amorphous with higher interplanar or interchain distance (3.5–3.6 Å). In the case of PANI-MeSA and PANI-*p*-TSA, higher doping level and smaller molecular size was of benefit for the close-packed arrangement of chains with improved crystallinity.

Cyclic voltammetry

The redox properties of the PANI salts were investigated with CV. Figure 4 showed the CVs of the polymer films on Pt in 1 mol/L H_2SO_4. Three redox couples are observed in the CVs of PANI-MeSA, PANI-*p*-TSA, and PANI-DBSA. The anodic and cathodic potentials are listed in Table VI. In the

TABLE VI
The Redox Potentials of PANI Salts

	I (first redox peak)		II (intermediate peaks)		III (second redox peak)	
Sample	E_{pa}/V	E_{pc}/V	E_{pa}/V	E_{pc}/V	E_{pa}/V	E_{pc}/V
PANI-DBSA	0.25	0.04	0.54	0.41	0.73	0.64
PANI-MeSA	0.25	0.12	0.52	0.45	0.73	0.62
PANI- *p*-TSA	0.21	0.07	0.48	0.40	0.68	0.60

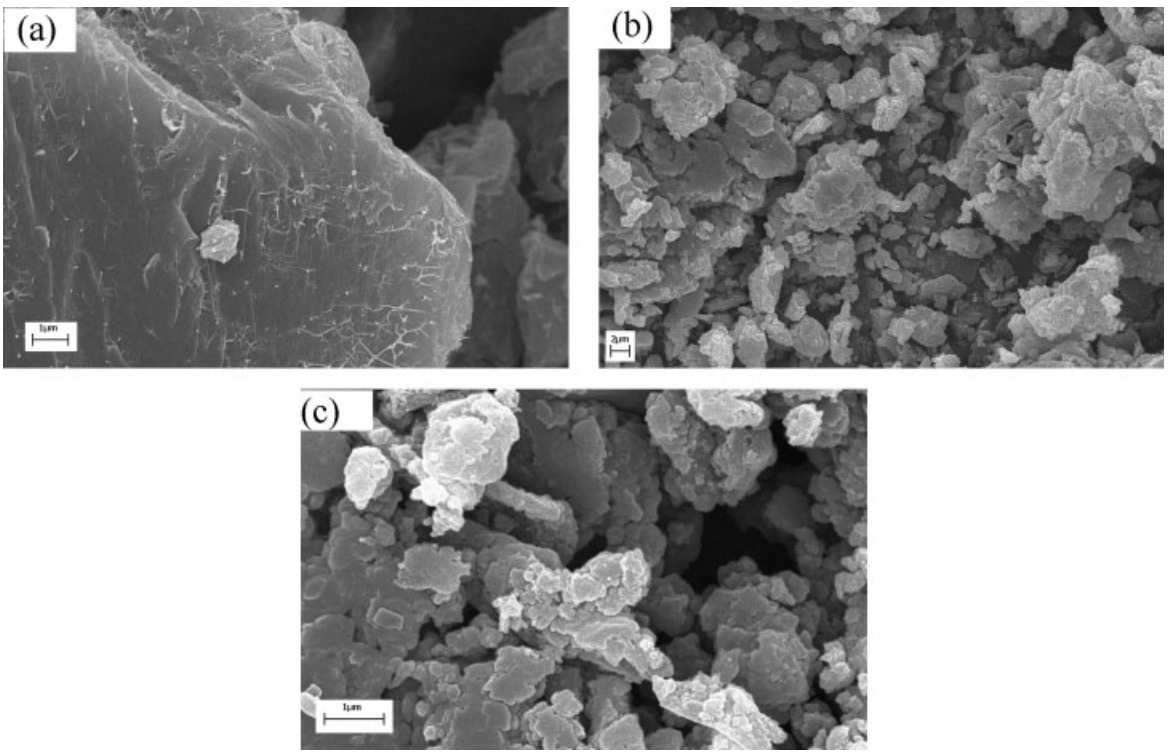

Figure 5 SEM images of (a) PANI-DBSA (original magnification = ×30,000), (b) PANI-MeSA (original magnification = ×8000), (c) PANI-*p*-TSA(original magnification = ×50,000).

positive sweep, the first redox peak (at ~ 0.21–0.25 V) was well known as the formation of radical cations (polaronic emeraldine)[35] and the second redox couple at ~ 0.68–0.73 V was the formation of diradical dications (represented by the resonance structures: bipolaronic pernigraniline and protonated quinonediimine)[36] through the oxidation of PANI salts. The intermediate peaks of relatively low intensity was absorbed between 0.48 and 0.54 V; these peaks were associated to the degradation of PANI salts.[37] One can see that the first anodic peaks were relatively sharp in CVs of PANI-MeSA and PANI-*p*-TSA. However, a broad first anodic peak was absorbed in the CV of PANI-DBSA. It is reported that the charge transfer becomes slower at longer oxidation times as can be seen from the increase in peak width at half height for first anodic peak,[18] so the broad first anodic peak in PANI-DBSA indicated that the PANI-DBSA had lower charge transferability.

Comparing with each other, some differences were observed in the redox peak potentials of PANI salts. Generally, the size of the counter anion plays an important role in the redox processes of PANI; the larger size of the acid anion increases the inter chain distance in the polymer membranes, resulting in a decrease in the electrical conductivity and an increase in the oxidation potential.[38] But in this study, the size of the acid anion alone cannot explain the electrochemical behavior of PANI-MeSA. If the size of the acid anion is the only controlling factor, then, compared with others, the first redox potential of PANI should shift to lower potential in the presence of MeSA, which was not so. This indicated that the interaction of the acid anion with PANI must be in the concern. Aromatic anions with delocalized π-electrons are likely to influence the π-conjugated polymer distinctly,[22] this may be the reason of the first redox potential of PANI shifted to lower potential in PANI-*p*-TSA than in PANI-MeSA with the π-electron delocalization between PANI and *p*-TSA, which favors for the higher charge transferring along the polymer chain. In the case PANI-DBSA, the longer interchain distance was presumably related to a lower interchain conductivity, and the role of π-electron delocalization between DBSA and PANI was not strong as the steric hindrance of longer alkyl chain tail, which caused the lower charge transferring by lower conductivity. Consequently, this increased the peak width at half height for first anodic peak. The lower reduction potential (E_{pc} = 0.04 V) that occurred in first redox process in PANI-DBSA also indicated lower charge transferring in reduction process.[38] This was well in accordance with the results described earlier.

Morphology

Figure 5 showed the SEM images of the PANI salts. As can be seen from Figure 5, PANI particles were

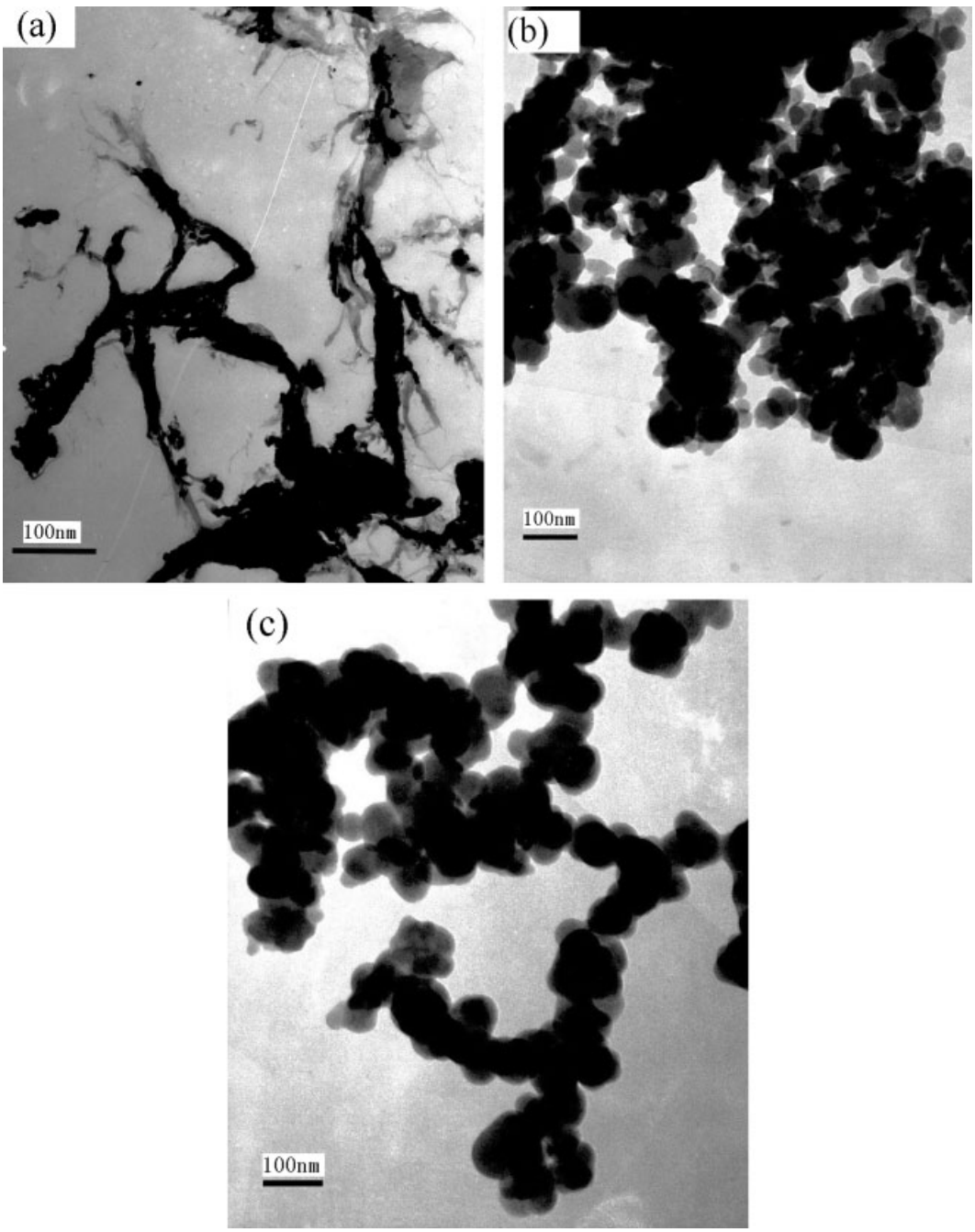

Figure 6 TEM images of (a) PANI-DBSA (original magnification = ×150000), (b) PANI-MeSA (original magnification = ×100000), (c) PANI-*p*-TSA (original magnification = ×100000).

irregularly shaped and aggregated. The particles were spherically shaped with comparatively smoother particle surface in PANI-*p*-TSA and PANI-MeSA, but their high tendency to aggregate hindered the recording of SEM images with perfectly spherical particles [Fig. 5(b,c)]. A comparison indicated that PANI-DBSA had remarkably different micromorphology. The particles were highly aggregated with lamellar structure, and the particle surface showed a fibrillar morphology, as shown in Figure 5(a), but no network was clearly observed.

TEM image [Fig. 6(a)] further proved that the fibril structure was really existence and the fibrils were at the submicrometer scale in the length PANI-DBSA. TEM images [Fig. 6(a,b)] also showed that the particles were actually spherically shaped in PANI-*p*-TSA, and these particles were at the nanoscale. This difference may be explained by the interaction between dopant and polymer chain. Among these organic sulfonic acids, for its longer alkyl tail, the DBSA doped in PANI increased the polymer chain interaction more stronger than other two organic

TABLE VII
The Conductivity values and yields of PANI salts

Sample	Conductivity (S/cm)	Yield (%)
PANI-DBSA	0.14	75
PANI-MeSA	0.90	60
PANI- *p*-TSA	1.25	81

sulfonic acids by secondary bonding (Van der Waals interaction), which may cause the high aggregation with lamellar structure in PANI-DBSA, since if the bond (secondary bonding) is too weak, it may energetically be more favorable to render macroscopic phase separation of particles. This may be the reason for less aggregation occurring in PANI-*p*-TSA and PANI-MeSA. For fibrillar morphology of PANI-DBSA, the possible reason may be the higher coiling tendency of longer alkyl tail of the DBSA with PANI chains, except the strong secondary bonding effect of alkyl tail of the DBSA. This would cause the coiling of polymer chain with DBSA and the intercoiling of alkyl tail of the DBSA, and this would favor the formation of fibrillar morphology in PANI-DBSA.

Yield and conductivity

The yield and conductivity of PANI salts obtained by solid-state polymerization are listed in Table VII. As far as the yield was concerned, PANI-MeSA had yield slightly lower than the others; this may be caused by smaller molecular weight. Even in the higher doping level, the produced PANI would be in slightly lower yield in MeSA; this was also the reason that yield of PANI was still high in the case of DBSA because of bigger molecular weight of DBSA.

From Table VII, one can see that the conductivity of PANI synthesized in *p*-TSA was the largest and that in DBSA is the smallest in these PANI salts. It is reported that the conductivity of PANI depends on the degree of doping, oxidation state, particle morphology, crystallinity, interor intrachain interactions, molecular weight, etc.[39–41]; that is, the conductivity of PANI increases with the increasing of doping degree and crystallinity, and the higher relative intensity of quinoid to benzenoid ring modes to that of doped anions in PANI will also bring a higher electrical conductivity of PANI. On the basis of these considerations, the differences in conductivity of these PANI salts could be explained by the results of IR spectra, UV–vis spectra, XRD analysis, and CV studies. These results showed that the emeraldine (half-oxidized form) type structure was predominant in PANI-*p*-TSA, and PANI-*p*-TSA had higher doping level and crstallinity. These could be the possible reasons for the higher conductivity of PANI-*p*-TSA, while lowest doping level and crystallinity resulted in the lower conductivity of PANI-DBSA.

CONCLUSIONS

PANI salts were synthesized by solid-state polymerization in different protonation media (MeSA, *p*-toluenesulphonic acid, and dodecylbenzenesulphonic acid). It was found that the dopants, such as methyl sulfonic acid, *p*-toluene sulfonic acid, and dodecylbenzenesulphonic acid, have different doping effect on physicochemical characteristics of PANI. Spectroscopic studies showed that highest ratio of the relative intensities of the quinoid to benzenoid unit in doped PANI and leucoemeraldine phase was formed predominantly in other PANI salts. These results were further supported by conductivity measurements and CV. A comparison indicated that among these PANI salts, *p*-TSA-doped PANI displayed higher doping level, crystallinity, eltrochemical activity, and conductivity, whereas the DBSA had the opposite effects on these properties of PANI. Morphology studies revealed that the fibril structured particles at the submicrometer scale in the length existed in PANI- DBSA, while PANI-*p*-TSA and PANI-MeSA were actually composed of fine particles at the nanoscale. These results indicated that the doping effect mainly depend on characteristics of organic sulfonic acids: different molecular structure, molecular size, acidity constants (p*Ka*), and solubility in water. In addition, the characteristics of solid-state polymerization method, in which the reaction happens only on the surface of reactant molecule, would also affect the physicochemical properties of PANI salts. All these factors resulted in different characteristics of PANI salts in solid-state polymerization.

References

1. MacDiarmid, A. G.; Chiang, J. C.; Richter, A. F.; Epstein, A. J. Synth Met 1987, 18, 285.
2. Geniès, E. M.; Boyle, A.; Lapkowski, M.; Tsintavis, C. Synth Met 1990, 36, 139.
3. Patil, A. O.; Heeger, A. J.; Wudl, F. Chem Rev 1988, 88, 183.
4. Novak, P.; Muller, K.; Santhanam, K. S. V.; Haas, O. Chem Rev 1997, 97, 207.
5. Paul; E. W.; Ricco, J. A.; Wrighton, M. S. J Phys Chem 1985, 89, 1441.
6. Sangodkar, H.; Sukeerthi, S.; Srinivasa, R. S.; Lal, R.; Contractor, A. Q. Anal Chem 1996, 68, 779.
7. Oyama, N.; Tatsuma, T.; Sato, T.; Sotomura, T. Nature 1995, 373, 598.
8. MacDiarmid, A. G.; Epstein, A. J. Faraday Discuss Chem Soc 1989, 88, 317.
9. Diaz, A. F.; Logan, J. A. J Electroanal Chem 1980, 111, 111.
10. MacDiarmid, A. G.; Chiang, J. C.; Halpern, M.; Huang, W. S.; Mu, S. L.; Somasiri, L. D.; Wu, W. Q.; Yaniger, S. I. Mol Cryst Liq Cryst 1985, 121, 173.

11. Huang, W. S.; Humphrey, B. D.; MacDiarmid, A. G. J Chem Soc Faraday Trans 1986, 82, 2385.
12. Gong, J.; Cui, X. J.; Xie, Z. W.; Wang, S. G.; Qu, L. Y. Synth Met 2002, 129, 187.
13. Acquaye, J. H.; Moore, J. A.; Huang, J. X.; Kaner, R. B. Polym Prepr (Am Chem Soc Div Polym Chem) 2004, 45, 147.
14. Huang, J.; Moore, J. A.; Acquaye, J. H.; Kaner, R. B. Macromolecules 2005, 38, 317.
15. Tursun, A.; Zhang, X. G.; Ruxangul, J. J Appl Polym Sci 2005, 96, 1630.
16. Milind, V. K.; Annamraju, K. V. Eur Polym J 2004, 40, 379.
17. Han, D. X.; Chu, Y.; Yang, L. K.; Liu, Y.; Zhongxian, L. V. Colloids Surf A 2005, 259, 179.
18. Vijiayan, M.; Trivedi, D. C. Synth Met 1999, 107, 57.
19. Milind, V. K.; Annamraju, K. V.; Marimuthu, R.; Tanay, S. J Polym Sci Part A: Polym Chem 2004, 42, 2043.
20. Gospodinova, N.; Terlemezyan, L. Prog Polym Sci 1998, 23, 1443.
21. Lee, D.; Char, K. Langmuir 2002, 18, 6445.
22. Tawde, S.; Mukesh, D.; Yakhmi, J. V. Synth Met 2001, 125, 401.
23. Epstein, A. J.; Ginder, J. M.; Zuo, F.; Bigelow, R. W.; Woo, H. S.; Tanner, D. B.; Richter, A. F.; Huang, W. S.; MacDiarmid, A. G. Synth Met 1987, 18, 303.
24. Wei, Y.; Hsuech, F. K.; Jang, G. W. Macromolecules 1994, 27, 518.
25. MacDiarmid, A. G.; Epstein, A. J. Synth Met 1994, 65, 103.
26. Xia, H. S.; Wang, Q. J. Nanopart Res 2001, 3, 401.
27. Cho, M. S.; Park, S. Y.; Hwang, J. Y.; Choi, H. J. Mater Sci Eng 2004, 24, 15.
28. de Souza, F. G., Jr.; B. G.Soares. Polym Test 2006, 25, 512.
29. Pouget, J. P.; Oblakowski, Z.; Nogami, Y.; Albony, P. A.; Laridiani, M.; Oh, E. J.; Min, Y.; MacDiarmid, A. G.; Tsukamuto, J.; Ishiguro, T.; Epstein, A. J. Synth Met 1994, 65, 131.
30. Moon, Y. B.; Cao, Y.; Smith, P.; Heeger, A. J. Polym Commun 1989, 30, 196.
31. Pouget, J. P.; Hsu, C. H.; MacDiarmid, A. G.; Epstein, A. J. Synth Met 1995, 69, 119.
32. Murugesan, R.; Subramanian, E. Mater Chem Phys 2004, 85, 184.
33. Pouget, J. P.; Jozefowicz, M. E.; Epstein, A. J.; Tang, X.; MacDiarmid, A. G. Macromolecules 1991, 24, 779.
34. Pouget, J. P.; Hsu, C. H.; MacDiarmid, A. G.; Epstein, A. J. Synth Met 1995, 69, 119.
35. Stilwell, D. E.; Park, S. M. J Electrochem Soc 1988, 135, 2254.
36. Yang, C. H.; Wen, T. C. J Appl Electrochem 1994, 24, 166.
37. Doic, L.; Mandic, Z. Electrochim Acta 1995, 40, 1681.
38. Lindfors, T.; Ivaska, A. J Electroanal Chem 2002, 531, 43.
39. Jiang, H.; Geng, Y.; Li, J.; Wang, F. Synth Met 1997, 84, 125.
40. Zhang, Z.; Wei, Z.; Wan, M. Macromolecules 2002, 35, 5937.
41. Mu, S. L.; Kan, J. Q. Synth Met 1998, 98, 51.